Available online at www.sciencedirect.com
ScienceDirect
Journal of Sound and Vibration 320 (2009) 649–667
JOURNAL OF SOUND AND VIBRATION
www.elsevier.com/locate/jsvi

Shear deformable versus classical theories for nonlinear vibrations of rectangular isotropic and laminated composite plates

M. Amabili[a,*], S. Farhadi[b]

[a]Dipartimento di Ingegneria Industriale, Università di Parma, Parco Area delle Scienze 181/A, Parma 43100, Italy
[b]Department of Mechanical Engineering, Iran University of Science and Technology, Narmak, Tehran 16846-13114, Iran

Received 8 May 2008; received in revised form 31 July 2008; accepted 7 August 2008
Handling Editor: A.V. Metrikine
Available online 19 September 2008

Abstract

In the present study, (i) the classical Von Kármán theory, (ii) the first-order shear deformation theory and (iii) the higher-order (third-order) shear deformation theory are compared for studying the nonlinear forced vibrations of isotropic and laminate composite rectangular plates. In particular, the harmonic response in the frequency neighborhood of the fundamental mode of rectangular plates is investigated and the response curves computed by using the three different theories are compared. The boundary conditions of the plates are simply supported with immovable edges. Geometric imperfections are taken into account. Calculations for isotropic and laminated composite plates are presented and results are discussed. For isotropic plates, the frequency-response curves for large-amplitude vibrations obtained by using the three theories are almost coincident. For laminated composite plates, differences arise for relatively thick plates (ratio between the thickness and the edge equal to 0.1), while for thin plates (ratio between the thickness and the edge equal to 0.01), no difference is obtained. For all cases, the first-order shear deformation (with shear correction factor $\sqrt{3}/2$) and the higher-order shear deformation theories give practically coincident results and differences are observed with respect to the classical Von Kármán theory.

1. Introduction

Classical and shear deformable theories are presented by Amabili [1] and Reddy [2]. A literature review of work on the nonlinear vibrations of plates is given by Chia [3,4] and Sathyamoorthy [5]. Nonlinear vibrations of plates have been studied using the classical Von Kármán nonlinear plate theory by many authors for isotropic and laminated composite plates, see, for example, Refs. [6–18].

*Corresponding author at: Dipartimento di Ingegneria Industriale, Università di Parma, Viale Usberti 181/A, Parma 43100, Italy. Tel.: +39 0521 905896; fax: +39 0521 905705.
E-mail address: marco.amabili@unipr.it (M. Amabili).
URL: http://me.unipr.it/mam/amabili/amabili.html (M. Amabili).

0022-460X/$ - see front matter © 2008 Elsevier Ltd. All rights reserved.
doi:10.1016/j.jsv.2008.08.006

In the case of moderately thick laminated plates, the classical plate theories can become inaccurate. In fact, the hypotheses of negligible shear deformation and rotary inertia for thick laminated shells can be a rough approximation. For laminated composite plates, because of the anisotropic material, there is a coupling between bending and stretching. The use of the Kirchhoff–Love hypothesis, which assumes that the normals to the middle surface after deformation remain straight and undergo no thickness stretching, gives rise to an overpredition of natural frequencies in laminated composite plates; this is due to neglecting shear strains and rotary inertia. For this reason, the nonlinear first-order shear deformation theory (SDT) and the nonlinear higher-order SDT have been used to study nonlinear vibrations of laminated plates, for example by Reddy and Chao [19], Reddy [20], Chen and Doong [21], Ganapathi et al. [22], Bhimaraddi [23], Rao et al. [24], Tenneti and Chandrashekhara [25], Singh et al. [26], Chen et al. [27], Huang and Zheng [28] and Chen et al. [29].

In the present study, (i) the classical Von Kárman theory, (ii) the first-order SDT and (iii) the higher-order (third-order) SDT are compared for studying the nonlinear forced vibrations of isotropic and laminate composite rectangular plates. In particular, the harmonic response in the frequency neighborhood of the fundamental mode of rectangular plates is investigated and the response curves computed by using the three different theories are compared. The boundary conditions of the plates are simply supported with immovable edges. Calculations for isotropic and laminated composite plates are presented and results are discussed. Geometric imperfections are taken into account. The aim of the present work is to find the area of applicability of the classical Von Kárman theory, which gives models with a reduced number of degrees of freedom (dofs) with respect to shear deformation theories, and applications where the use of shear deformation theories is necessary to obtain accurate results.

2. Shear deformable theories

2.1. Nonlinear first-order SDT

The nonlinear first-order SDT of plates, introduced by Reddy and Chao [19], is presented. Five independent variables, three displacements u, v and w and two rotations ϕ_1 and ϕ_2, are used to describe the plate's middle plane deformation; the geometric imperfection w_0 in the normal direction is also introduced. This theory may be regarded as the thick-plate version of the Von Kárman theory since the nonlinear terms are the same.

A laminated rectangular plate of thickness h, made of a finite number of orthotropic layers oriented arbitrarily with respect to the plate orthogonal coordinate system (x, y, z), is considered. The coordinate system is chosen such that x and y lie on the middle surface, which is obtained for $z = 0$, and are parallel to the edges; the coordinate z is taken perpendicular to the middle surface.

The hypotheses are (i) the transverse normal stress σ_z is negligible; in general, it is verified that σ_z is small compared with τ_{xz} and τ_{yz}, except near the edges, so that the hypothesis is a good approximation of the actual behavior of moderately thick plates and (ii) the normal to the middle surface of the plate before deformation remains straight, but not necessarily normal, after deformation; this is a relaxed version of the Kirchhoff hypothesis.

The displacements u_1, u_2, u_3 of a generic point at distance z from the middle plane (see Fig. 1) are related to the middle surface displacements u, v, w by

$$u_1 = u + z\phi_1, \quad u_2 = v + z\phi_2, \quad u_3 = w + w_0, \tag{1a–c}$$

where ϕ_1 and ϕ_2 are the rotations of the transverse normals about the y and x axes, respectively, and w_0 is the geometrical imperfection in the z direction. A higher-order (in z) displacement field can be assumed in Eqs. (1a–c); however, a linear field in z is assumed for the first-order SDT. In Eq. (1c), it is assumed that the normal displacement is constant through the thickness, which means that $\varepsilon_Z = 0$ is assumed.

The strain–displacement equations for the first-order SDT are given by [1]

$$\varepsilon_x = \varepsilon_{x,0} + z\, k_x^{(0)}, \tag{2a}$$

$$\varepsilon_y = \varepsilon_{y,0} + z\, k_y^{(0)}, \tag{2b}$$

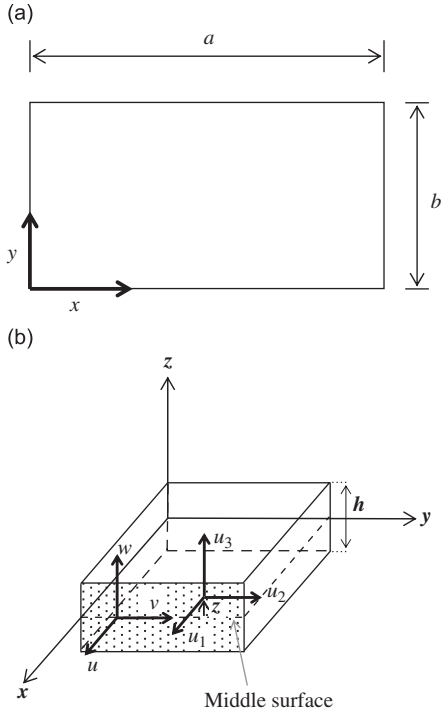

Fig. 1. Rectangular plate: (a) coordinates and dimensions and (b) symbols used for displacements of middle surface and a generic point.

$$\gamma_{xy} = \gamma_{xy,0} + z\, k_{xy}^{(0)}, \tag{2c}$$

$$\gamma_{xz} = \gamma_{xz,0}, \tag{2d}$$

$$\gamma_{yz} = \gamma_{yz,0}, \tag{2e}$$

where

$$\varepsilon_{x,0} = \frac{\partial u}{\partial x} + \frac{1}{2}\left(\frac{\partial w}{\partial x}\right)^2 + \frac{\partial w}{\partial x}\frac{\partial w_0}{\partial x}, \tag{3a}$$

$$\varepsilon_{y,0} = \frac{\partial v}{\partial y} + \frac{1}{2}\left(\frac{\partial w}{\partial y}\right)^2 + \frac{\partial w}{\partial y}\frac{\partial w_0}{\partial y}, \tag{3b}$$

$$\gamma_{xy,0} = \frac{\partial u}{\partial y} + \frac{\partial v}{\partial x} + \frac{\partial w}{\partial x}\frac{\partial w}{\partial y} + \frac{\partial w}{\partial x}\frac{\partial w_0}{\partial y} + \frac{\partial w_0}{\partial x}\frac{\partial w}{\partial y}, \tag{3c}$$

$$\gamma_{xz,0} = \phi_1 + \frac{\partial w}{\partial x}, \tag{3d}$$

$$\gamma_{yz,0} = \phi_2 + \frac{\partial w}{\partial y}, \tag{3e}$$

$$k_x^{(0)} = \frac{\partial \phi_1}{\partial x}, \tag{3f}$$

$$k_y^{(0)} = \frac{\partial \phi_2}{\partial y}, \tag{3g}$$

$$k_{xy}^{(0)} = \frac{\partial \phi_1}{\partial y} + \frac{\partial \phi_2}{\partial x}. \tag{3h}$$

Eqs. (2d,e) show a uniform distribution of shear strains through the shell thickness, which gives uniform shear stresses. The top and bottom surfaces of the shell can clearly not support shear stresses; therefore, the result is only a first approximation. The actual distribution of shear stresses is close to a parabolic distribution through the thickness, taking zero value at the top and bottom surfaces. For this reason, for equilibrium considerations, it is necessary to introduce a shear correction factor with the first-order SDT in order not to overestimate the shear forces.

2.2. Nonlinear higher-order SDT

A nonlinear, higher-order SDT of plates has been introduced by Reddy [30]. The reason for introducing this theory is to overcome the limit of the uniform shear strain and stress distribution through the thickness, obtained with the first-order SDT. A discussion about different formulations of nonlinear higher-order shear deformation theories for plates and their equivalence is given by Reddy [31]

A laminated rectangular plate, made of a finite number of orthotropic layers, oriented arbitrarily with respect to the plate coordinate system (x, y, z), is considered; however, the theory is unchanged for isotropic and functionally graded materials. The displacements of a generic point are related to the middle surface displacements by

$$u_1 = u + z\phi_1 + z^2\psi_1 + z^3\gamma_1 + z^4\theta_1, \tag{4a}$$

$$u_2 = v + z\phi_2 + z^2\psi_2 + z^3\gamma_2 + z^4\theta_2, \tag{4b}$$

$$u_3 = w + w_0, \tag{4c}$$

where ϕ_1 and ϕ_2 are the rotations of the transverse normals at $z = 0$ about the y and x axes, respectively, and the other terms can be computed as functions of w, ϕ_1 and ϕ_2. After satisfying the zero shear strains at $z = \pm h/2$, see Amabili [1], the following expressions are obtained:

$$u_1 = u + z\phi_1 - \frac{4}{3h^2}z^3\left(\phi_1 + \frac{\partial w}{\partial x}\right), \tag{5a}$$

$$u_2 = v + z\phi_2 - \frac{4}{3h^2}z^3\left(\phi_2 + \frac{\partial w}{\partial y}\right), \tag{5b}$$

$$u_3 = w + w_0, \tag{5c}$$

where the geometric imperfection w_0 in the normal direction has been introduced. Eqs. (5a,b) represent the parabolic distribution of shear effects through the thickness and satisfy the zero shear boundary condition at both the top and bottom surfaces of the plate. This is the justification for the use of a third-order SDT.

The strain–displacement equations for the higher-order SDT, keeping the terms up to z^3, can be written as [1]

$$\varepsilon_x = \varepsilon_{x,0} + z(k_x^{(0)} + z^2 k_x^{(2)}), \tag{6a}$$

$$\varepsilon_y = \varepsilon_{y,0} + z(k_y^{(0)} + z^2 k_y^{(2)}), \tag{6b}$$

$$\gamma_{xy} = \gamma_{xy,0} + z(k_{xy}^{(0)} + z^2 k_{xy}^{(2)}), \tag{6c}$$

$$\gamma_{xz} = \gamma_{xz,0} + z(z k_{xz}^{(1)}), \tag{6d}$$

$$\gamma_{yz} = \gamma_{yz,0} + z(z k_{yz}^{(1)}), \tag{6e}$$

where

$$\varepsilon_{x,0} = \frac{\partial u}{\partial x} + \frac{1}{2}\left(\frac{\partial w}{\partial x}\right)^2 + \frac{\partial w}{\partial x}\frac{\partial w_0}{\partial x}, \tag{7a}$$

$$\varepsilon_{y,0} = \frac{\partial v}{\partial y} + \frac{1}{2}\left(\frac{\partial w}{\partial y}\right)^2 + \frac{\partial w}{\partial y}\frac{\partial w_0}{\partial y}, \tag{7b}$$

$$\gamma_{xy,0} = \frac{\partial v}{\partial x} + \frac{\partial u}{\partial y} + \frac{\partial w}{\partial x}\frac{\partial w}{\partial y} + \frac{\partial w}{\partial x}\frac{\partial w_0}{\partial y} + \frac{\partial w_0}{\partial x}\frac{\partial w}{\partial y}, \tag{7c}$$

$$\gamma_{xz,0} = \phi_1 + \frac{\partial w}{\partial x}, \tag{7d}$$

$$\gamma_{yz,0} = \phi_2 + \frac{\partial w}{\partial y}, \tag{7e}$$

$$k_x^{(0)} = \frac{\partial \phi_1}{\partial x}, \tag{8a}$$

$$k_x^{(2)} = -\frac{4}{3h^2}\left(\frac{\partial \phi_1}{\partial x} + \frac{\partial^2 w}{\partial x^2}\right), \tag{8b}$$

$$k_y^{(0)} = \frac{\partial \phi_2}{\partial y}, \tag{8c}$$

$$k_y^{(2)} = -\frac{4}{3h^2}\left(\frac{\partial \phi_2}{\partial y} + \frac{\partial^2 w}{\partial y^2}\right), \tag{8d}$$

$$k_{xy}^{(0)} = \frac{\partial \phi_1}{\partial y} + \frac{\partial \phi_2}{\partial x}, \tag{8e}$$

$$k_{xy}^{(2)} = -\frac{4}{3h^2}\left(\frac{\partial \phi_1}{\partial y} + \frac{\partial \phi_2}{\partial x} + 2\frac{\partial^2 w}{\partial x \partial y}\right), \tag{8f}$$

$$k_{xz}^{(1)} = -\frac{4}{h^2}\gamma_{xz,0}, \quad k_{yz}^{(1)} = -\frac{4}{h^2}\gamma_{yz,0}. \tag{8g,h}$$

2.3. Elastic strain energy for laminated plates

The stress–strain relations for the kth orthotropic lamina of the plate, in the material principal coordinates, under the hypothesis $\sigma_3 = 0$, are given by

$$\begin{Bmatrix} \sigma_1 \\ \sigma_2 \\ \tau_{23} \\ \tau_{13} \\ \tau_{12} \end{Bmatrix}^{(k)} = \begin{bmatrix} c_{11} & c_{12} & 0 & 0 & 0 \\ c_{21} & c_{22} & 0 & 0 & 0 \\ 0 & 0 & G_{23} & 0 & 0 \\ 0 & 0 & 0 & G_{13} & 0 \\ 0 & 0 & 0 & 0 & G_{12} \end{bmatrix}^{(k)} \begin{Bmatrix} \varepsilon_1 \\ \varepsilon_2 \\ \gamma_{23} \\ \gamma_{13} \\ \gamma_{12} \end{Bmatrix}, \tag{9}$$

where G_{12}, G_{13} and G_{23} are the shear moduli in 1–2, 1–3 and 2–3 directions, respectively, and the coefficients c_{ij} are given in Appendix A; τ_{13} and τ_{23} are the shear stresses and the superscript (k) refers to the kth layer within a laminate. Eq. (9) is obtained (i) under the transverse isotropy assumption with respect to planes parallel to

the 2–3 plane, i.e., assuming fibers in the direction parallel to axis 1, so that $E_2 = E_3$, $G_{12} = G_{13}$ and $v_{12} = v_{13}$, and (ii) solving the constitutive equations for ε_3 as a function of ε_1 and ε_2 and then eliminating it.

Eq. (9) can be transformed to the plate coordinates (x, y, z) by the following vectorial equation:

$$\begin{Bmatrix} \sigma_x \\ \sigma_y \\ \tau_{yz} \\ \tau_{xz} \\ \tau_{xy} \end{Bmatrix}^{(k)} = [Q]^{(k)} \begin{Bmatrix} \varepsilon_x \\ \varepsilon_y \\ \gamma_{yz} \\ \gamma_{xz} \\ \gamma_{xy} \end{Bmatrix}, \tag{10}$$

where $[Q]^{(k)}$ is the 5×5 matrix of the material properties of the kth layer transformed in the plate principal coordinates and it is given in Appendix A. In particular, Eq. (10) can be written as

$$\begin{Bmatrix} \sigma_x \\ \sigma_y \\ \tau_{yz} \\ \tau_{xz} \\ \tau_{xy} \end{Bmatrix}^{(k)} = [Q]^{(k)} \begin{Bmatrix} \varepsilon_{x,0} \\ \varepsilon_{y,0} \\ \gamma_{yz,0} \\ \gamma_{xz,0} \\ \gamma_{xy,0} \end{Bmatrix} + z[Q]^{(k)} \begin{Bmatrix} k_x^{(0)} \\ k_y^{(0)} \\ 0 \\ 0 \\ k_{xy}^{(0)} \end{Bmatrix} + z^2[Q]^{(k)} \begin{Bmatrix} 0 \\ 0 \\ k_{yz}^{(1)} \\ k_{xz}^{(1)} \\ 0 \end{Bmatrix} + z^3[Q]^{(k)} \begin{Bmatrix} k_x^{(2)} \\ k_y^{(2)} \\ 0 \\ 0 \\ k_{xy}^{(2)} \end{Bmatrix} \tag{11}$$

for the first-order SDT, the terms in z^2 and z^3 do not appear.

The elastic strain energy U_P of the plate is given by

$$U_P = \frac{1}{2}\sum_{k=1}^{K} \int_0^a \int_0^b \int_{h^{(k-1)}}^{h^{(k)}} \left(\sigma_x^{(k)}\, \varepsilon_x + \sigma_y^{(k)}\, \varepsilon_y + \tau_{xy}^{(k)}\, \gamma_{xy} + K_x^2 \tau_{xz}^{(k)}\, \gamma_{xz} + K_y^2 \tau_{yz}^{(k)}\, \gamma_{yz} \right) \mathrm{d}x\, \mathrm{d}y\, \mathrm{d}z, \tag{12}$$

where K is the total number of layers in the laminated shell, a and b are the in-plane dimensions, $(h^{(k-1)}, h^{(k)})$ are the z coordinates of the kth layer and K_x and K_y the shear correction factors, which are equal to one (no correction) for the higher-order SDT. The shear correction factor used in the present calculations for the first-order SDT is $K_x^2 = K_y^2 = \sqrt{3}/2$.

2.4. Kinetic energy with rotary inertia for laminated plates

The kinetic energy T_P of the plate, including rotary inertia, is given by

$$T_P = \frac{1}{2}\sum_{k=1}^{K} \rho_P^{(k)} \int_0^a \int_0^b \int_{h^{(k-1)}}^{h^{(k)}} (\dot{u}_1^2 + \dot{u}_2^2 + \dot{u}_3^2)\, \mathrm{d}x\, \mathrm{d}y\, \mathrm{d}z, \tag{13}$$

where $\rho_P^{(k)}$ is the mass density of the kth layer of the plate and the overdot denotes the time derivative. For the first-order SDT, Eq. (13) becomes

$$T_P = \frac{1}{2}\sum_{k=1}^{K} \rho_P^{(k)} \int_0^a \int_0^b \int_{h^{(k-1)}}^{h^{(k)}} \{\dot{u}^2 + \dot{v}^2 + \dot{w}^2 + z[2\dot{\phi}_1\dot{u} + 2\dot{\phi}_2\dot{v}] + z^2[\dot{\phi}_1^2 + \dot{\phi}_2^2]\}\, \mathrm{d}x\, \mathrm{d}y\, \mathrm{d}z. \tag{14}$$

The z term vanishes after integration on z in the case of a laminate with symmetric density with respect to the z-axis.

For the higher-order SDT, Eq. (13) becomes

$$\begin{aligned} T_P = \frac{1}{2}\sum_{k=1}^{K} \rho_P^{(k)} \int_0^a \int_0^b \int_{h^{(k-1)}}^{h^{(k)}} \Big\{ & \dot{u}^2 + \dot{v}^2 + \dot{w}^2 + z[2\dot{\phi}_1\dot{u} + 2\dot{\phi}_2\dot{v}] + z^2[\dot{\phi}_1^2 + \dot{\phi}_2^2] \\ & + z^3\left[-2\frac{4}{3h^2}\dot{u}\left(\dot{\phi}_1 + \frac{\partial \dot{w}}{\partial x}\right) - 2\frac{4}{3h^2}\dot{v}\left(\dot{\phi}_2 + \frac{\partial \dot{w}}{\partial y}\right)\right] + O(z^4)\Big]\Big\} \mathrm{d}x\, \mathrm{d}y\, \mathrm{d}z, \end{aligned} \tag{15}$$

where $O(z^4)$ are small terms compared with z^2; the z and z^3 terms vanish after integration on z in the case of a laminate with symmetric density with respect to the z-axis.

3. Boundary conditions and discretization

In order to reduce the system to finite dimensions, the middle surface displacements u, v and w are expanded using approximate functions.

A specific boundary conditions is analyzed in the present study: simply supported plate with immovable edges. The boundary conditions for the simply supported plate with immovable edges are as follows:

$$u = v = w = \phi_2 = w_0 = M_x = \partial^2 w_0/\partial x^2 = 0 \quad \text{at } x = 0, a, \tag{16a–g}$$

$$u = v = w = \phi_1 = w_0 = M_y = \partial^2 w_0/\partial y^2 = 0 \quad \text{at } y = 0, b, \tag{17a–g}$$

where M_x and M_y are the bending moment per unit length.

The following base of panel displacements, which satisfy identically the geometric boundary conditions (16a–d) and (17a–d), is used to discretize the system:

$$u(x, y, t) = \sum_{m=1}^{M}\sum_{n=1}^{N} u_{2m,n}(t)\sin(2m\pi x/a)\sin(n\pi y/b), \tag{18a}$$

$$v(x, y, t) = \sum_{m=1}^{M}\sum_{n=1}^{N} v_{m,2n}(t)\sin(m\pi x/a)\sin(2n\pi y/b), \tag{18b}$$

$$w(x, y, t) = \sum_{m=1}^{\hat{M}}\sum_{n=1}^{\hat{N}} w_{m,n}(t)\sin(m\,\pi\, x/a)\sin(n\pi y/b), \tag{18c}$$

$$\phi_1(x, y, t) = \sum_{m=1}^{\hat{M}}\sum_{n=1}^{\hat{N}} \phi_{1_{m,n}}(t)\cos(m\pi x/a)\sin(n\pi y/b), \tag{18d}$$

$$\phi_2(x, y, t) = \sum_{m=1}^{\hat{M}}\sum_{n=1}^{\hat{N}} \phi_{2_{m,n}}(t)\sin(m\pi x/a)\cos(n\pi y/b), \tag{18e}$$

where m and n are the numbers of half-waves in x and y directions, respectively, and t is the time; $u_{m,n}(t)$, $v_{m,n}(t)$, $w_{m,n}(t)$, $\phi_{1_{m,n}}(t)$ and $\phi_{2_{m,n}}(t)$ are the generalized coordinates that are unknown functions of t. M and N indicate the terms necessary in the expansion of the in-plane displacements and, in general, are larger than $\hat{M}$ and $\hat{N}$, respectively, which indicate the terms in the expansion of out-of-plane displacement and rotations. By using a different number of terms in the expansions, it is possible to study the convergence and the accuracy of the solution.

Initial geometric imperfections of the rectangular plate are considered only in the z direction. They are assumed to be associated with zero initial stress. The imperfection w_0 is expanded in the same form as w, that is, in a double Fourier sine series satisfying the boundary conditions (16e,g) and (17e,g) at the plate edges

$$w_0(x, y) = \sum_{m=1}^{\tilde{M}}\sum_{n=1}^{\tilde{N}} A_{m,n}\sin(m\pi x/a)\sin(n\pi y/b), \tag{19}$$

where $A_{m,n}$ are the modal amplitudes of imperfections; $\tilde{N}$ and $\tilde{M}$ are integers indicating the number of terms in the expansion.

The boundary conditions 16(f) and 17(f) can be transformed into

$$M_x = \sum_{k=1}^{K}\int_{h^{(k-1)}}^{h^{(k)}} \sigma_x^{(k)} z\,\mathrm{d}\,z = 0 \quad \text{at } x = 0,\ a, \tag{20a}$$

$$M_y = \sum_{k=1}^{K} \int_{h^{(k-1)}}^{h^{(k)}} \sigma_y^{(k)} z \, \mathrm{d}z = 0 \quad \text{at } y = 0,\ b, \tag{20b}$$

where the stresses σ_x and σ_y, which are functions of z and of the different material properties in each layer of the laminate, are related to the strains by Eqs. (10) and (11). For the given expressions of $k_x^{(0)}$, $k_x^{(2)}$, $k_y^{(0)}$and $k_y^{(2)}$, which are all zero at $x = 0$, a and $y = 0$, b for the given expansions (18a–e), Eqs. (20a,b) are identically satisfied for symmetric laminates. Additional terms must be added to expansions of the in-plane displacements u and v for asymmetric laminates in order to satisfy exactly Eqs. (20a,b), as shown in Appendix B. In fact, bending and stretching are coupled for asymmetric laminates.

4. Lagrange equations of motion

The virtual work W done by the external forces is written as

$$W = \int_0^a \int_0^b (q_x u + q_y v + q_z w) \, \mathrm{d}x \, \mathrm{d}y, \tag{21}$$

where q_x, q_y and q_z are the distributed forces per unit area acting in x, y and z directions, respectively, applied at the middle surface. Only a single harmonic force orthogonal to the plate is considered; therefore, $q_x = q_y = 0$. The external distributed load q_z applied to the plate, due to the normal concentrated force $\tilde{f}$, is given by

$$q_z = \tilde{f} \delta(x - \tilde{x}) \delta(y - \tilde{y}) \cos(\omega t), \tag{22}$$

where ω is the excitation frequency, t is the time, δ is the Dirac delta function, $\tilde{f}$ gives the force magnitude positive in the z direction and $\tilde{x}$ and $\tilde{y}$ give the position of the point of application of the force. Here, the point excitation is located at the center of the plate, that is, $\tilde{x} = a/2$, $\tilde{y} = b/2$. Eq. (21) can be rewritten in the following form:

$$W = \tilde{f} \cos(\omega t)(w)_{x=a/2,\ y=b/2}. \tag{23}$$

The nonconservative damping forces are assumed to be of the viscous type and are taken into account by using the Rayleigh dissipation function:

$$F = \frac{1}{2} c \int_0^a \int_0^b (\dot{u}^2 + \dot{v}^2 + \dot{w}^2 + \dot{\phi}_1^2 + \dot{\phi}_2^2) \, \mathrm{d}x \, \mathrm{d}y, \tag{24}$$

where c has a different value for each term of the mode expansion, in particular

$$F = \frac{1}{2} \frac{ab}{4} \left[\sum_{n=1}^{N} \sum_{m=1}^{M} c_{m,n} \frac{\dot{u}_{m,n}^2 + \dot{v}_{m,n}^2}{h^2} + \sum_{n=1}^{\hat{N}} \sum_{m=1}^{\hat{M}} c_{m,n} \left(\frac{\dot{w}_{m,n}^2}{h^2} + \dot{\phi}_{1_{m,n}}^2 + \dot{\phi}_{2_{m,n}}^2 \right) \right]. \tag{25}$$

In Eq. (25), displacements are nondimensionalized dividing by h, while rotations are already nondimensional. The damping coefficient $c_{m,n}$ is related to the modal damping ratio that can be evaluated from experiments by $\zeta_{m,n} = c_{m,n}/(2\mu_{m,n}\,\omega_{m,n})$, where $\omega_{m,n}$ is the natural circular frequency of mode (m, n) and $\mu_{m,n}$ is the modal mass of this mode.

The following notation is introduced for brevity:

$$\mathbf{q} = \{u_{m,n}, v_{m,n}, w_{m,n}, \phi_{1_{m,n}}, \phi_{2_{m,n}}\}^{\mathrm{T}},\ m = 1, \ldots, M \text{ or } \hat{M} \quad \text{and} \quad n = 1, \ldots, N \text{ or } \hat{N}. \tag{26}$$

The generic element of the time-dependent vector q is referred to as q_j; the dimension of q is $\bar{N}$, which is the number of dofs used in the mode expansion.

The generalized forces Q_j are obtained by differentiation of the Rayleigh dissipation function and of the virtual work done by external forces:

$$Q_j = -\frac{\partial F}{\partial \dot{q}_j} + \frac{\partial W}{\partial q_j}. \tag{27}$$

The Lagrange equations of motion are

$$\frac{\mathrm{d}}{\mathrm{d}t}\left(\frac{\partial T_P}{\partial \dot{q}_j}\right)-\frac{\partial T_P}{\partial q_j}+\frac{\partial U_P}{\partial q_j}=Q_j,\quad j=1,\ldots,\bar{N}, \tag{28}$$

where $\partial T_P/\partial q_j=0$. The complicated term, derived from the maximum potential energy of the plate, giving quadratic and cubic nonlinearities, can be written in the form

$$\frac{\partial U}{\partial q_j}=\sum_{i=1}^{\bar{N}} f_{j,i}q_i+\sum_{i,k=1}^{\bar{N}} f_{j,i,k}q_iq_k+\sum_{i,k,l=1}^{\bar{N}} f_{j,i,k,l}q_iq_kq_l,\quad j=1,\ldots,\bar{N}, \tag{29}$$

where the coefficients f have long expressions that include also geometric imperfections. It is interesting to observe that in Eq. (29) there are quadratic and cubic terms. In particular, quadratic terms appear in all the equations of motion as a consequence of including in-plane generalized coordinates. If the simpler Von Kármán equation of motion is used neglecting in-plane inertia, only cubic nonlinearities are obtained for perfectly flat plates. The presence of quadratic nonlinearities in the discretized equations of motion lead to the appearance of second-order harmonic components in response to harmonic excitation in the neighborhood of a plate resonance. Third-order harmonics are due to cubic nonlinearities and are obtained both retaining and neglecting in-plane inertia. In the presence of geometric imperfections, plates become shallow shells; due to the curvature of the middle surface, stronger second-order harmonics appear.

4.1. Inertial coupling in the equations of motion

For plates with rotary inertia, inertial coupling arises in the equations of motion (see Eq. (15)) so that they cannot be immediately transformed in the form required for numerical integration. In particular, the equations of motion take the following form:

$$\mathbf{M}\ddot{\mathbf{q}}+\mathbf{C}\dot{\mathbf{q}}+[\mathbf{K}+\mathbf{N}_2(\mathbf{q})+\mathbf{N}_3(\mathbf{q},\mathbf{q})]\mathbf{q}=\mathbf{f}_0\cos(\omega t), \tag{30}$$

where $\mathbf{M}$ is the nondiagonal mass matrix of dimension $\bar{N}\times\bar{N}$ ($\bar{N}$ being the number of dofs), $\mathbf{C}$ the damping matrix, $\mathbf{K}$ the linear stiffness matrix, which does not present terms involving $\mathbf{q}$, $\mathbf{N}_2$ the matrix that involves linear terms in $\mathbf{q}$, therefore giving the quadratic nonlinear stiffness terms, $\mathbf{N}_3$ the matrix that involves quadratic terms in $\mathbf{q}$, therefore giving the cubic nonlinear stiffness terms, $\mathbf{f}_0$ the vector of excitation amplitudes and $\mathbf{q}$ the vector of the $\bar{N}$ generalized coordinates, defined in Eq. (26). In particular, by using Eq. (29), the generic elements $k_{j,i}$, $n_{2_{j,i}}$ and $n_{3_{j,i}}$, of the matrices $\mathbf{K}$, $\mathbf{N}_2$ and $\mathbf{N}_3$, respectively, are given by

$$k_{j,i}=f_{j,i},\quad n_{2_{j,i}}(\mathbf{q})=\sum_{k=1}^{\bar{N}} f_{j,i,k}q_k,\quad n_{3_{j,i}}(\mathbf{q},\mathbf{q})=\sum_{k,l=1}^{\bar{N}} f_{j,i,k,l}q_kq_l \tag{31a–c}$$

Eq. (30) is pre-multiplied by $\mathbf{M}^{-1}$ in order to diagonalize the mass matrix, as a consequence matrix $\mathbf{M}$ is always invertible; the result is

$$\mathbf{I}\ddot{\mathbf{q}}+\mathbf{M}^{-1}\mathbf{C}\dot{\mathbf{q}}+[\mathbf{M}^{-1}\mathbf{K}+\mathbf{M}^{-1}\mathbf{N_2}(\mathbf{q})+\mathbf{M}^{-1}\mathbf{N_3}(\mathbf{q},\mathbf{q})]\mathbf{q}=\mathbf{M}^{-1}\mathbf{f_0}\cos(\omega t), \tag{32}$$

which can be rewritten in the following form:

$$\mathbf{I}\ddot{\mathbf{q}}+\tilde{\mathbf{C}}\dot{\mathbf{q}}+[\tilde{\mathbf{K}}+\mathbf{M}^{-1}\mathbf{N}_2(\mathbf{q})+\mathbf{M}^{-1}\mathbf{N}_3(\mathbf{q},\mathbf{q})]\mathbf{q}=\tilde{\mathbf{f}}_0\cos(\omega t), \tag{33}$$

where

$$\tilde{\mathbf{C}}=\mathbf{M}^{-1}\mathbf{C},\quad \tilde{\mathbf{K}}=\mathbf{M}^{-1}\mathbf{K}\quad\text{and}\quad \tilde{\mathbf{f}}_0=\mathbf{M}^{-1}\mathbf{f}_0. \tag{34a–c}$$

Eq. (33) is in the form suitable for numerical integration.

5. Numerical results

Calculations have been performed for harmonic excitation applied at the center of square plates, having the following dimensions $a=b=0.3\,\mathrm{m}$; the excitation frequency has been kept around the natural frequency of

the fundamental mode ($m = 1$, $n = 1$). The boundary conditions are simply supported, immovable edges. In Section 5.1, isotropic plates are considered, while laminated plates are studied in Section 5.2. Calculations have been performed by using the computer program AUTO [32] based on the pseudo-arclength continuation method.

5.1. Isotropic plates

Aluminum square plates are considered with the following dimensions and material properties: $a = b = 0.3\,\text{m}$, $E = 70\,\text{GPa}$, $\rho = 2778\,\text{kg/m}^3$ and $\nu = 0.3$. Initially, a plate with thickness $h = 0.001\,\text{m}$ ($h/a = 0.0033$) is considered. The natural frequency of the fundamental mode, computed by using classical and shear deformation theories, is given in Table 1.

The response of the plate to harmonic force excitation $\tilde{f} = 1.74\,\text{N}$ in the neighborhood of the circular frequency $\omega_{1,1}$ of the fundamental mode is presented in Fig. 2. The response has been obtained by using the third-order SDT, assuming a modal damping ratio $\zeta = 0.065$ for all the generalized coordinates and by using a model with 24 degrees of freedom (dofs). In particular, the model with 24 dofs includes the following generalized coordinates: $w_{1,1}$, $w_{3,1}$, $w_{1,3}$, $w_{3,3}$, $\phi_{1_{1,1}}$, $\phi_{1_{3,1}}$, $\phi_{1_{1,3}}$, $\phi_{1_{3,3}}$,$\phi_{2_{1,1}}$, $\phi_{2_{3,1}}$, $\phi_{2_{1,3}}$, $\phi_{2_{3,3}}$, $u_{2,1}$, $u_{4,1}$, $u_{6,1}$, $u_{8,1}$, $u_{2,3}$, $u_{4,3}$, $v_{1,2}$, $v_{1,4}$, $v_{1,6}$, $v_{1,8}$, $v_{3,2}$, $v_{3,4}$. Results show a strong hardening-type nonlinearity. The same results have been obtained in Fig. 3 by using the first-order SDT. In particular, in Fig. 3, a model with 24 dofs is compared with a reduced model with 15 dofs, giving practically coincident results. The following generalized coordinates are

Table 1
Natural frequency (Hz) of the fundamental mode (1,1) of the square plate $a = b = 0.3\,\text{m}$ computed by using the classical Von Kármán theory, and first- and third-order shear deformation theories (SDT)

Material	h/a	Von Kármán	First-order SDT	Third-order SDT
Aluminum	0.0033	53.025	53.023	53.023
Aluminum	0.1	1590.7	1537.9	1536.4
Laminated	0.01	100.22	99.940	99.926
Laminated	0.1	1002.22	808.53	801.47

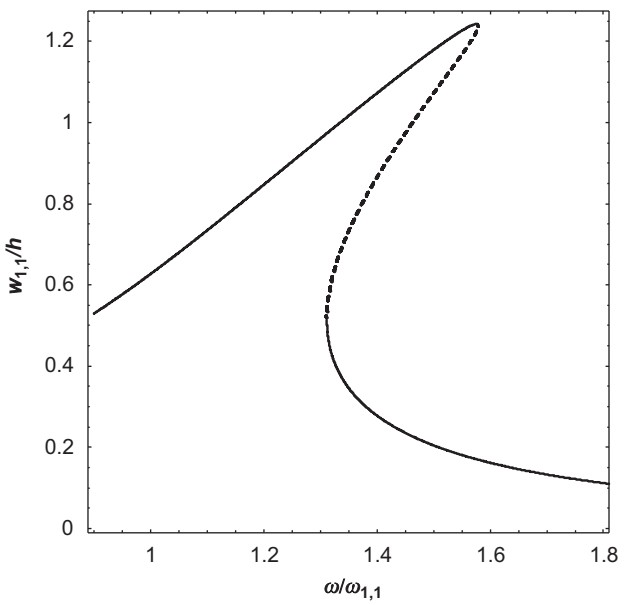

Fig. 2. Frequency-response behavior for the third-order shear deformation theory; $h/a = 0.0033$, $\tilde{f} = 1.74\,\text{N}$, $\zeta_{1,1} = 0.065$ and 24 dofs. ——, stable solutions; - -, unstable solutions.

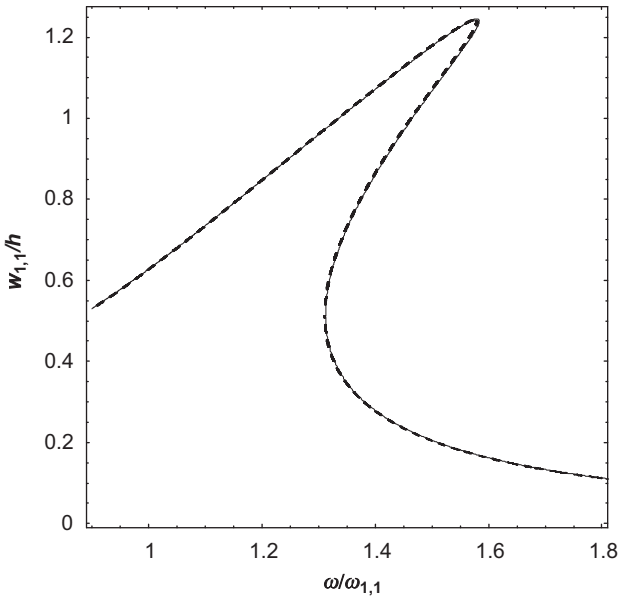

Fig. 3. Convergence of the frequency-response curve for the first-order shear deformation theory; $h/a = 0.0033$, $\tilde{f} = 1.74\,\mathrm{N}$ and $\zeta_{1,1} = 0.065$. ——, 15 dofs; - -, 24 dofs.

used in the 15 dofs model: $w_{1,1}$, $\phi_{1_{1,1}}$, $\phi_{2_{1,1}}$, $u_{2,1}$, $u_{4,1}$, $u_{6,1}$, $u_{8,1}$, $u_{2,3}$, $u_{4,3}$, $v_{1,2}$, $v_{1,4}$, $v_{1,6}$, $v_{1,8}$, $v_{3,2}$, $v_{3,4}$; i.e., only one term is used for w, ϕ_1 and ϕ_2. For this plate, the response computed by using the Von Kármán, first-order and third-order shear deformation theories is practically coincident. Results for the Von Kármán theory have been previously obtained by Amabili [17] for this case, and are in perfect agreement with those obtained by Ribeiro [14] and Chu and Hermann [6]. According to the Von Kármán theory, the trend of nonlinearity is not affected by the thickness ratio h/a; however, it is affected according to the shear deformation theories. Therefore, it is expected to find differences among the plate theories by increasing the thickness ratio h/a.

In the following calculations, the 15 dofs model (13 dofs for the the Von Kármán theory) is used and a plate with increased thickness $h = 0.03\,\mathrm{m}$ ($h/a = 0.1$) is considered. The excitation force has been increased in order to keep the same nondimensionalized value $\tilde{f}/(h\omega_{1,1}^2\mu_{1,1}) = 0.249$ of the previous cases. The natural frequency of the fundamental mode is given in Table 1, where the value computed by using the Von Kármán theory is about 3.5% higher than the value obtained by using shear deformation theories with rotary inertia. The comparison of the responses computed by using the Von Kármán, first-order and third-order shear deformation theories is presented in Figs. 4 and 5. Results obtained by the two theories with shear deformation are coincident, as shown in Fig. 4, but results by the classical Von Kármán theory are very close, as shown in Fig. 5.

In order to compare the three plate theories for larger vibration amplitudes, the damping ratio is divided by two in Fig. 6 ($\zeta = 0.0325$). Also in this case, results obtained by the two theories with shear deformation are coincident, while the results from the Von Kármán theory are close.

5.2. Laminated plates

Calculations have been performed for a graphite/epoxy $(0^\circ/90^\circ)_S$ symmetric laminated plate with dimensions $a = b = 0.3\,\mathrm{m}$ and the following material properties of each layer: $\rho = 1000\,\mathrm{kg/m^3}$, $E_1 = 40\,\mathrm{GPa}$, $E_2 = 1\,\mathrm{GPa}$, $G_{12} = G_{13} = 0.6\,\mathrm{GPa}$, $G_{23} = 0.5\,\mathrm{GPa}$ and $\nu_{12} = 0.25$.

Initially, a plate with thickness $h = 0.03\,\mathrm{m}$ ($h/a = 0.1$) is considered. The natural frequency of the fundamental mode, computed by using classical and shear deformation theories, is given in Table 1, where the value computed by using the Von Kármán theory is about 25% higher than the value obtained by using shear deformation theories with rotary inertia.

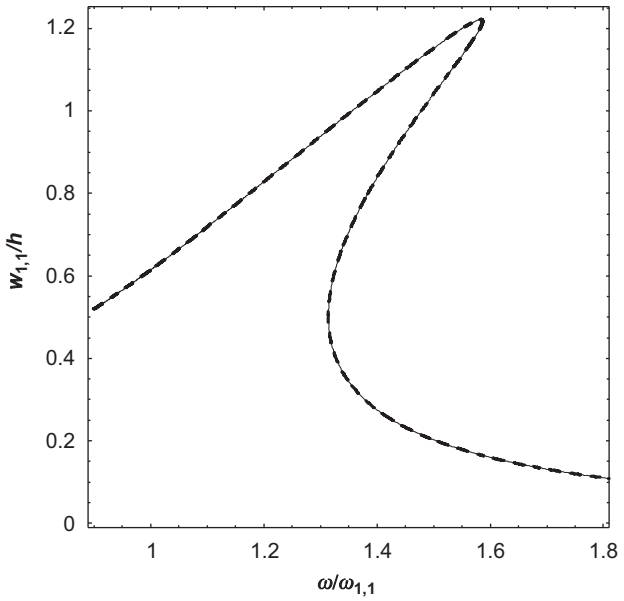

Fig. 4. Comparison of the frequency-response curves computed by using the first-order and the third-order shear deformation theories; $h/a = 0.1$, $\tilde{f} = 1.31 \times 10^6$ N, $\zeta_{1,1} = 0.065$ and 15 dofs. ——, First-order shear deformation theory; - -, third-order shear deformation theory.

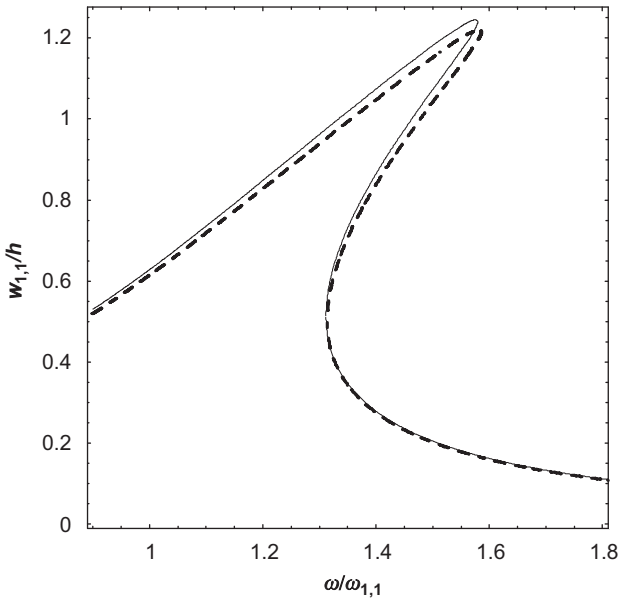

Fig. 5. Comparison of the frequency-response curves computed by using the Von Kárman and the third-order shear deformation theories; $h/a = 0.1$, $\tilde{f} = 1.31 \times 10^6$ N, $\zeta_{1,1} = 0.065$ and 15 dofs. ——, Von Kárman theory;- -, third-order shear deformation theory.

The response of the plate to harmonic force excitation in the neighborhood of the circular frequency $\omega_{1,1}$ of the fundamental mode is presented in Fig. 7. The response has been obtained by using the three different theories, assuming a modal damping ratio $\zeta = 0.0325$ for all the generalized coordinates and by using a model with 24 dofs for the two shear deformation theories and 16 dofs for the Von Kárman theory. It must be observed that all the dofs related to rotations ϕ_1 and ϕ_2 must be eliminated for the Von Kárman theory. The excitation force has been chosen in order to have the same nondimensionalized value of the previous cases of

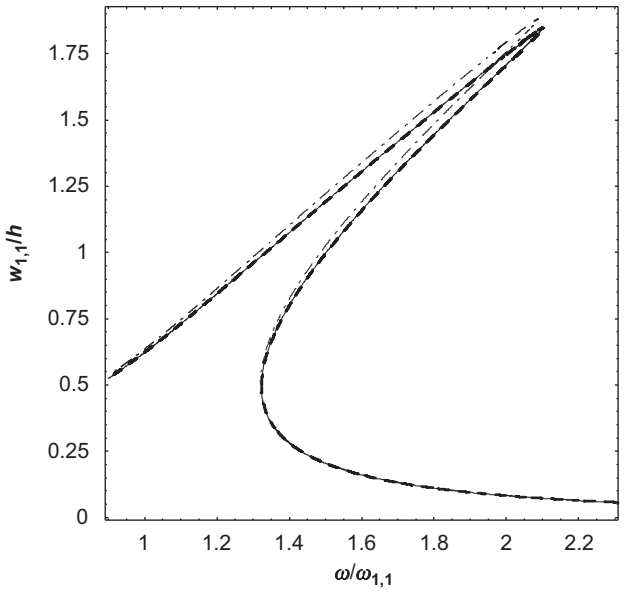

Fig. 6. Comparison of the frequency-response curves computed by using Von Kárman, first-order and third-order shear deformation theories; $h/a = 0.1$, $\tilde{f} = 1.31 \times 10^6$ N, $\zeta_{1,1} = 0.0325$ and 15 dofs. – ● –, Von Kárman theory; ——, first-order shear deformation theory; – –, third-order shear deformation theory.

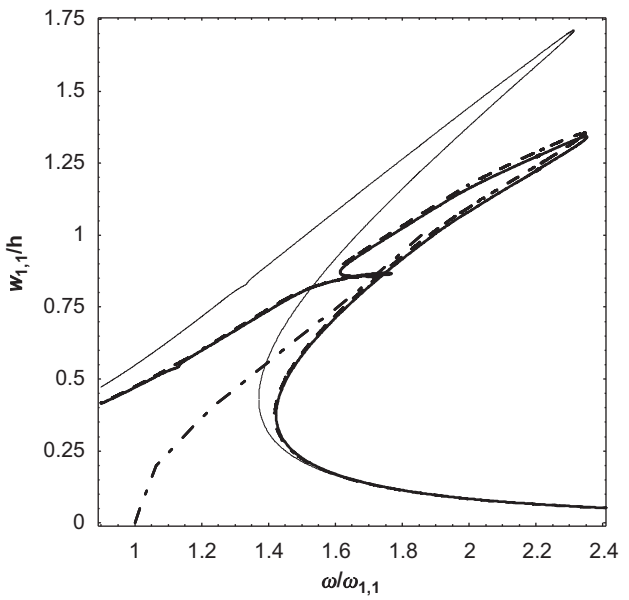

Fig. 7. Comparison of the frequency-response curves computed by using Von Kárman, first-order and third-order shear deformation theories for laminated plate; $h/a = 0.1$, $\tilde{f} = 128 \times 10^3$ N, $\zeta_{1,1} = 0.0325$ and 24 dofs (16 dofs for the Von Kárman theory). ——, Von Kárman theory; – –, first-order shear deformation theory; ——, third-order shear deformation theory; – ● –, backbone curve from Ref. [22].

isotropic plates. Results in Fig. 7 obtained by using the two shear deformation theories are extremely close; however, the results from the Von Kárman theory are not accurate enough. Moreover, the responses computed by using the shear deformation theories show a deviation from the single-mode hardening-type behavior for excitation around $1.6 \times \omega_{1,1}$. In fact, three 3:1 internal resonances arise between modes (3,1), (1,3) and (3,3) with mode (1,1) in the frequency range around the fundamental resonance; in particular, at $1.6 \times \omega_{1,1}$ there is an internal resonance between modes (1,1) and (3,3). No internal resonances are detected by using the

Von Kármán theory since it gives an inaccurate evaluation of the natural frequencies. A good agreement is found between the response computed by using shear deformable theories and the backbone curve reported by Ganapathi et al. [22] for the same case shown in Fig. 7; results in Ref. [22] were obtained by using the first-order SDT.

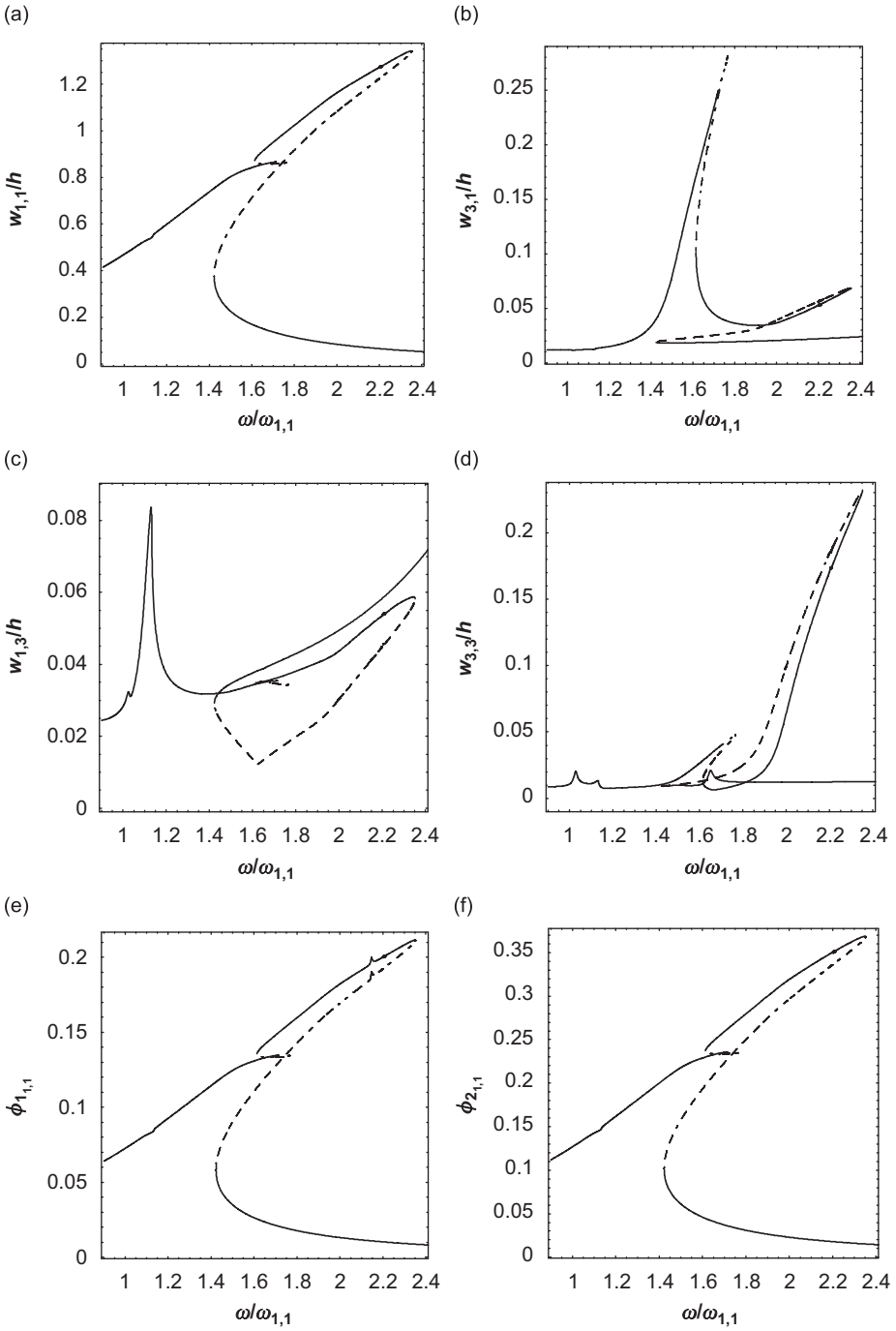

Fig. 8. Frequency-response curves computed by using the third-order shear deformation theories for the laminated plate; $h/a = 0.1$, $\tilde{f} = 128 \times 10^3$ N, $\zeta_{1,1} = 0.0325$ and 24 dofs. ——, Stable solutions; – –, unstable solutions: (a) generalized coordinate $w_{1,1}$; (b) generalized coordinate $w_{3,1}$; (c) generalized coordinate $w_{1,3}$; (d) generalized coordinate $w_{3,3}$; (e) generalized coordinate $\phi_{1_{1,1}}$ and (f) generalized coordinate $\phi_{2_{1,1}}$.

The internal resonances are investigated in Fig. 8(a–f), where the main generalized coordinates are shown. In particular, the generalized coordinate $w_{3,3}$ is shown in Fig. 8(d) and presents a response amplitude largely increasing for excitation frequency larger than $1.6 \times \omega_{1,1}$. Actually the generalized coordinate $w_{3,1}$, see Fig. 8(b), presents a response peak at $1.6 \times \omega_{1,1}$, but the 3:1 internal resonance between modes (1,1) and (3,1) is at $1.33 \times \omega_{1,1}$. The generalized coordinate $w_{1,3}$, see Fig. 8(c), presents a response peak, of smaller amplitude with respect to the other coordinates involving w, at $1.1 \times \omega_{1,1}$ (but the internal resonance is at $0.98 \times \omega_{1,1}$). Therefore, there is a strong interaction among the generalized coordinates $w_{1,1}$, $w_{3,1}$, $w_{1,3}$ and $w_{3,3}$ in the frequency range in the neighborhood of the fundamental frequency.

The same laminated plate with reduced thickness $h = 0.003$ m ($h/a = 0.01$) is considered in Fig. 9. For this thin plate, the Von Kármán and shear deformation theories give almost coincident results.

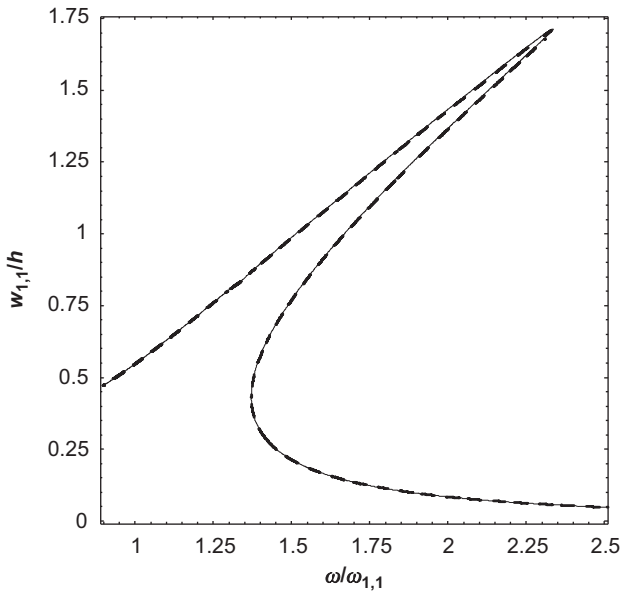

Fig. 9. Comparison of the frequency-response curves computed by using Von Kármán and third-order shear deformation theories for laminated plate; $h/a = 0.01$, $\tilde{f} = 19.9$ N, $\zeta_{1,1} = 0.0325$ and 24 dofs (16 dofs for the Von Kármán theory). ——, Von Kármán theory; – –, third-order shear deformation theory.

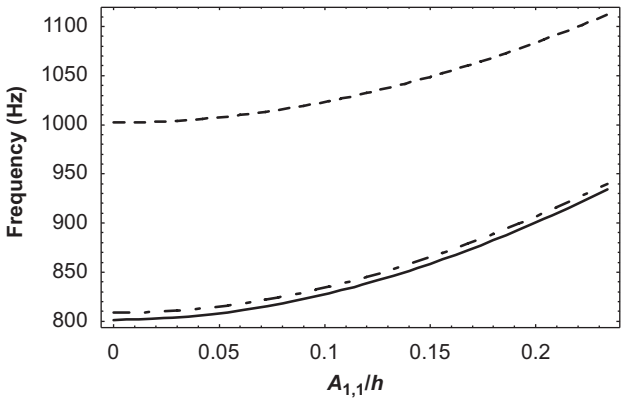

Fig. 10. Effect of geometric imperfection $A_{1,1}$ on the natural frequency of the fundamental mode of the laminated plate; $h/a = 0.1$, 24 dofs (16 dofs for the Von Kármán theory). – –, Von Kármán theory; – ● –, first-order shear deformation theory; ——, third-order shear deformation theory.

Geometric imperfection $A_{1,1}$ with the same shape of the fundamental mode is introduced to the laminated plate with thickness $h = 0.03$ m. The effect of this imperfection on the natural frequency of the fundamental mode is shown in Fig. 10; the frequency is rapidly increasing for imperfections larger than 0.05 times the plate thickness h.

6. Conclusions

Results show that for isotropic plates, some percent difference (3.5% for $h/a = 0.1$ in the present case) is obtained in the calculation of the natural frequency of the fundamental mode between classical and shear deformation theories. However, nonlinear results are very close. This indicates that it is not recommended to use a shear deformable theory with rotary inertia to evaluate the nonlinear response of isotropic moderately thick plates (at least up to $h/a = 0.1$ for the fundamental mode) since they require additional dofs to take into account the two additional variables ϕ_1 and ϕ_2 related to rotations. Eventually, it may be convenient to correct the linear part of the Von Kárman equation to obtain a correct evaluation of the natural frequency.

For laminated plates, the differences are increased at the point that for $h/a = 0.1$ it is highly recommended to use a shear deformable theory with rotary inertia to calculate the nonlinear response. However, for thin laminated plates ($h/a \leqslant 0.01$), the classical Von Kárman theory should be applied since it allows a reduced size of the model, at least for the laminated plates investigated; this may not be true in general, particularly for sandwich plates [35,36]. Between the first-order (with shear correction factor $\sqrt{3}/2$) and the third-order shear deformation theories, no appreciable differences are found for all the calculations. Moreover, the two theories require the same number of dofs and computational effort.

The relatively small differences among nonlinear responses computed by using the three theories of plates may be explained since the nonlinear terms are the same for all the three theories.

Appendix A. Stress–strain relations for a layer within a laminate

The coefficients in Eq. (9) for a lamina are given by

$$c_{11} = \frac{E_1}{1 - \nu_{12}\nu_{21}}, \quad c_{12} = c_{21} = \frac{E_2\nu_{12}}{1 - \nu_{12}\nu_{21}}, \quad c_{22} = \frac{E_2}{1 - \nu_{12}\nu_{21}}, \quad \nu_{ij}E_j = \nu_{ji}E_i. \tag{A.1}$$

Usually, the lamina material axes (1,2) do not coincide with the plate reference axes (x,y), while the 3 axis is coincident with z. Then, the strains and stresses on material axes can be related to the reference axes by using the following invertible expressions [33]:

$$\begin{Bmatrix} \sigma_1 \\ \sigma_2 \\ \tau_{23} \\ \tau_{13} \\ \tau_{12} \end{Bmatrix} = \mathbf{T}_1 \begin{Bmatrix} \sigma_x \\ \sigma_y \\ \tau_{yz} \\ \tau_{xz} \\ \tau_{xy} \end{Bmatrix}, \quad \begin{Bmatrix} \varepsilon_1 \\ \varepsilon_2 \\ \gamma_{23} \\ \gamma_{13} \\ \gamma_{12} \end{Bmatrix} = \mathbf{T}_2 \begin{Bmatrix} \varepsilon_x \\ \varepsilon_y \\ \gamma_{yz} \\ \gamma_{xz} \\ \gamma_{xy} \end{Bmatrix}, \tag{A.2a,b}$$

where

$$\mathbf{T}_1 = \begin{bmatrix} \cos^2\theta & \sin^2\theta & 0 & 0 & 2\sin\theta\cos\theta \\ \sin^2\theta & \cos^2\theta & 0 & 0 & -2\sin\theta\cos\theta \\ 0 & 0 & \cos\theta & -\sin\theta & 0 \\ 0 & 0 & \sin\theta & \cos\theta & 0 \\ -\sin\theta\cos\theta & \sin\theta\cos\theta & 0 & 0 & \cos^2\theta - \sin^2\theta \end{bmatrix}, \tag{A.3}$$

$$\mathbf{T}_2 = \begin{bmatrix} \cos^2\theta & \sin^2\theta & 0 & 0 & \sin\theta\cos\theta \\ \sin^2\theta & \cos^2\theta & 0 & 0 & -\sin\theta\cos\theta \\ 0 & 0 & \cos\theta & -\sin\theta & 0 \\ 0 & 0 & \sin\theta & \cos\theta & 0 \\ -2\sin\theta\cos\theta & 2\sin\theta\cos\theta & 0 & 0 & \cos^2\theta-\sin^2\theta \end{bmatrix}. \tag{A.4}$$

It can be shown that [34]

$$(\mathbf{T}_1^{-1})^{\mathrm{T}} = \mathbf{T}_2. \tag{A.5}$$

Therefore, the matrix $[Q]^{(k)}$ in Eqs. (10) and (11) is given by

$$[Q]^{(k)} = [\mathbf{T}_1^{-1}\mathbf{C}(\mathbf{T}_1^{-1})^{\mathrm{T}}]^{(k)}, \tag{A.6}$$

where $\mathbf{C}$ is the 5×5 matrix of coefficients c_{ij} in Eqs. (9) and (A.1). As a consequence of the discontinuous variation of the stiffness matrix $[Q]^{(k)}$ from layer to layer, the stresses may be discontinuous layer to layer.

Appendix B. Additional terms for asymmetric laminates

Using Eq. (11), boundary conditions (20a,b) can be rewritten in the following form:

$$M_x = \sum_{k=1}^{K}\int_{h^{(k-1)}}^{h^{(k)}} \left\{Q_{11}^{(k)}, Q_{12}^{(k)}, Q_{13}^{(k)}, Q_{14}^{(k)}, Q_{15}^{(k)}\right\} \cdot \left(\begin{Bmatrix} \varepsilon_{x,0} \\ \varepsilon_{y,0} \\ \gamma_{yz,0} \\ \gamma_{xz,0} \\ \gamma_{xy,0} \end{Bmatrix} z + \begin{Bmatrix} k_x^{(0)} \\ k_y^{(0)} \\ 0 \\ 0 \\ k_{xy}^{(0)} \end{Bmatrix} z^2 + \begin{Bmatrix} 0 \\ 0 \\ k_{yz}^{(1)} \\ k_{xz}^{(1)} \\ 0 \end{Bmatrix} z^3 + \begin{Bmatrix} k_x^{(2)} \\ k_y^{(2)} \\ 0 \\ 0 \\ k_{xy}^{(2)} \end{Bmatrix} z^4 \right) \mathrm{d}z = 0$$

at $x = 0,\ a$, (B.1)

$$M_y = \sum_{k=1}^{K}\int_{h^{(k-1)}}^{h^{(k)}} \left\{Q_{21}^{(k)}, Q_{22}^{(k)}, Q_{23}^{(k)}, Q_{24}^{(k)}, Q_{25}^{(k)}\right\} \cdot \left(\begin{Bmatrix} \varepsilon_{x,0} \\ \varepsilon_{y,0} \\ \gamma_{yz,0} \\ \gamma_{xz,0} \\ \gamma_{xy,0} \end{Bmatrix} z + \begin{Bmatrix} k_x^{(0)} \\ k_y^{(0)} \\ 0 \\ 0 \\ k_{xy}^{(0)} \end{Bmatrix} z^2 + \begin{Bmatrix} 0 \\ 0 \\ k_{yz}^{(1)} \\ k_{xz}^{(1)} \\ 0 \end{Bmatrix} z^3 + \begin{Bmatrix} k_x^{(2)} \\ k_y^{(2)} \\ 0 \\ 0 \\ k_{xy}^{(2)} \end{Bmatrix} z^4 \right) \mathrm{d}z = 0$$

at $y = 0,\ b$. (B.2)

In order to satisfy exactly boundary conditions (B.1) and (B.2) for asymmetric laminates, it is necessary to introduce additional terms $\hat{u}$ and $\hat{v}$ in Eqs. (18a,b), respectively. These additional terms $\hat{u}$ and $\hat{v}$ are second-order terms in the displacement w (linear terms are not considered since they are satisfied by energy minimization). Eliminating linear terms (since their contribution is satisfied by energy minimization), in each layer of an asymmetric laminated plate, the following expressions should be satisfied:

$$\left[\frac{\partial\hat{u}}{\partial x} + \frac{Q_{15}^{(k)}}{Q_{11}^{(k)}}\frac{\partial\hat{v}}{\partial x} - \frac{1}{2}\left(\frac{\partial w}{\partial x}\right)^2 - \frac{\partial w}{\partial x}\frac{\partial w_0}{\partial x}\right]_{x=0,a} = 0, \tag{B.3}$$

$$\left[\frac{\partial\hat{v}}{\partial y} + \frac{Q_{25}^{(k)}}{Q_{22}^{(k)}}\frac{\partial\hat{u}}{\partial y} - \frac{1}{2}\left(\frac{\partial w}{\partial y}\right)^2 - \frac{\partial w}{\partial y}\frac{\partial w_0}{\partial y}\right]_{y=0,b} = 0. \tag{B.4}$$

By inserting Eqs. (18c) and (19) into (B.3) and (B.4), two differential equations in $\hat{u}$ and $\hat{v}$ are obtained. The terms $\hat{u}$ and $\hat{v}$ are

$$\hat{u} = \frac{1}{2}\sum_{m=1}^{\hat{M}}\sum_{n=1}^{\hat{N}}\sum_{i=1}^{\hat{M}}\sum_{j=1}^{\hat{N}} w_{mn}w_{ij}\frac{(nj)\pi}{(n+j)a}\sin\frac{(n+j)\pi x}{a}\sin\frac{m\pi y}{b}\sin\frac{i\pi y}{b} + \sum_{m=1}^{\hat{M}}\sum_{n=1}^{\hat{N}}\sum_{i=1}^{\tilde{M}}\sum_{j=1}^{\tilde{N}} w_{mn}A_{ij}\frac{(nj)\pi}{(n+j)a}\sin\frac{(n+j)\pi x}{a}\sin\frac{m\pi y}{b}\sin\frac{i\pi y}{b}, \tag{B.5}$$

$$\hat{v} = \frac{1}{2}\sum_{m=1}^{\hat{M}}\sum_{n=1}^{\hat{N}}\sum_{i=1}^{\hat{M}}\sum_{j=1}^{\hat{N}} w_{mn}w_{ij}\frac{(mi)\pi}{(m+i)b}\sin\frac{(m+i)\pi y}{b}\sin\frac{n\pi x}{a}\sin\frac{j\pi x}{a} + \sum_{m=1}^{\hat{M}}\sum_{n=1}^{\hat{N}}\sum_{i=1}^{\tilde{M}}\sum_{j=1}^{\tilde{N}} w_{mn}A_{ij}\frac{(mi)\pi}{(m+i)b}\sin\frac{(m+i)\pi y}{b}\sin\frac{n\pi x}{a}\sin\frac{j\pi x}{a}. \tag{B.6}$$

References

[1] M. Amabili, *Nonlinear Vibrations and Stability of Shells and Plates*, Cambridge University Press, New York, USA, 2008.
[2] J.N. Reddy, *Mechanics of Laminated Composite Plates*, CRC Press, Boca Raton, FL, USA, 1997.
[3] C.-Y. Chia, *Nonlinear Analysis of Plates*, McGraw-Hill, New York, USA, 1980.
[4] C.-Y. Chia, Geometrically nonlinear behavior of composite plates: a review, *Applied Mechanics Reviews* 41 (1988) 439–451.
[5] M. Sathyamoorthy, Nonlinear vibration analysis of plates: a review and survey of current developments, *Applied Mechanics Reviews* 40 (1987) 1553–1561.
[6] H.-N. Chu, G. Herrmann, Influence of large amplitude on free flexural vibrations of rectangular elastic plates, *Journal of Applied Mechanics* 23 (1956) 532–540.
[7] D. Hui, Effects of geometric imperfections on frequency–load interaction of biaxially compressed antisymmetric angle ply rectangular plates, *Journal of Applied Mechanics* 52 (1985) 155–162.
[8] A.Y.T. Leung, S.G. Mao, A symplectic Galerkin method for non-linear vibration of beams and plates, *Journal of Sound and Vibration* 183 (1995) 475–491.
[9] A. Abe, Y. Kobayashi, G. Yamada, Two-mode response of simply supported, rectangular laminated plates, *International Journal of Non-linear Mechanics* 33 (1998) 675–690.
[10] W. Han, M. Petyt, Geometrically nonlinear vibration analysis of thin, rectangular plates using the hierarchical finite element method—I: the fundamental mode of isotropic plates, *Computers and Structures* 63 (1997) 295–308.
[11] W. Han, M. Petyt, Geometrically nonlinear vibration analysis of thin, rectangular plates using the hierarchical finite element method—II: 1st mode of laminated plates and higher modes of isotropic and laminated plates, *Computers and Structures* 63 (1997) 309–318.
[12] P. Ribeiro, M. Petyt, Geometrical non-linear, steady-state, forced, periodic vibration of plate, part I: model and convergence study, *Journal of Sound and Vibration* 226 (1999) 955–983.
[13] P. Ribeiro, M. Petyt, Geometrical non-linear, steady-state, forced, periodic vibration of plate, part II: stability study and analysis of multi-modal response, *Journal of Sound and Vibration* 226 (1999) 985–1010.
[14] P. Ribeiro, Periodic vibration of plates with large displacements. *Proceedings of the 42nd AIAA/ASME/ASCE/AHS/ASC Structures, Structural Dynamics, and Material Conference and Exhibit*, Seattle, WA, USA, 2001, Paper A01-25098.
[15] C. Touzé, O. Thomas, A. Chaigne, Asymmetric non-linear forced vibrations of free-edge circular plates—part 1: theory, *Journal of Sound and Vibration* 258 (2002) 649–676.
[16] B. Harras, R. Benamar, R.G. White, Geometically non-linear free vibration of fully clamped symmetrically laminated rectangular composite plates, *Journal of Sound and Vibration* 251 (2002) 579–619.
[17] M. Amabili, Nonlinear vibrations of rectangular plates with different boundary conditions: theory and experiments, *Computers and Structures* 82 (2004) 2587–2605.
[18] M. Amabili, Theory and experiments for large-amplitude vibrations of rectangular plates with geometric imperfections, *Journal of Sound and Vibration* 291 (2006) 539–565.
[19] J.N. Reddy, W.C. Chao, Large-deflection and large-amplitude free vibrations of laminated composite-material plates, *Computers and Structures* 13 (1981) 341–347.
[20] J.N. Reddy, Geometrically nonlinear transient analysis of laminated composite plates, *AIAA Journal* 21 (1983) 621–629.
[21] L.W. Chen, J.L. Doong, Large amplitude vibration of an initially stressed moderately thick plate, *Journal of Sound and Vibration* 89 (1983) 499–508.

[22] M. Ganapathi, T.K. Varadan, B.S. Sarma, Nonlinear flexural vibrations of laminated orthotropic plates, *Computers and Structures* 39 (1991) 685–688.
[23] A. Bhimaraddi, Large amplitude vibrations of imperfect antisymmetric angle-ply laminated plates, *Journal of Sound and Vibration* 162 (1993) 457–470.
[24] S.R. Rao, A.H. Sheikh, M. Mukhopadhyay, Large-amplitude finite element flexural vibration of plates/stiffened plates, *Journal of the Acoustical Society of America* 93 (1993) 3250–3257.
[25] R. Tenneti, K. Chandrashekhara, Large amplitude flexural vibration of laminated plates using a higher order shear deformation theory, *Journal of Sound and Vibration* 176 (1994) 279–285.
[26] G. Singh, G.V. Rao, N.G.R. Iyengar, Finite element analysis of the non-linear vibration of moderately thick unsymmetric laminated composite plates, *Journal of Sound and Vibration* 181 (1995) 315–329.
[27] C.-S. Chen, J.R. Hwang, J.L. Doong, Nonlinear vibration of an initially stressed plate based on a modified plate theory, *International Journal of Solids and Structures* 38 (2001) 8563–8583.
[28] X.-L. Huang, J.-J. Zheng, Nonlinear vibration and dynamic response of simply supported shear deformable laminated plates on elastic foundations, *Engineering Structures* 25 (2003) 1107–1119.
[29] C.-S. Chen, C.-P. Fung, R.-D. Chien, Nonlinear vibration of an initially stressed laminated plate according to a higher-order theory, *Composite Structures* 77 (2007) 521–532.
[30] J.N. Reddy, A refined nonlinear theory of plates with transverse shear deformation, *International Journal of Solids and Structures* 20 (1984) 881–896.
[31] J.N. Reddy, A general non-linear third-order theory of plates with moderate thickness, *International Journal of Non-linear Mechanics* 25 (1990) 677–686.
[32] E.J. Doedel, A.R. Champneys, T.F. Fairgrieve, Y.A. Kuznetsov, B. Sandstede, X. Wang, *AUTO 97: Continuation and Bifurcation Software for Ordinary Differential Equations (with HomCont)*, Concordia University, Montreal, Canada, 1998.
[33] J.E. Ashton, J.M. Whitney, *Theory of Laminated Plates*, Technomic, Stamford, CT, USA, 1970.
[34] A.K. Nayak, S.S.J. Moy, R.A. Shenoi, Free vibration analysis of composite sandwich plates based on Reddy's higher-order theory, *Composites: Part B* 33 (2002) 505–519.
[35] E. Carrera, S. Brischetto, A survey with numerical assessment of classical and refined theories for the analysis of sandwich plates, *Applied Mechanics Reviews* (2008), in press.
[36] L. Demasi, 2D, quasi 3D and 3D exact solutions for bending of thick and thin sandwich plates, *Journal of Sandwich Structures and Materials* 10 (2008) 271–310.